SUPERNOVA MODELS

S. E. Woosley*+

Board of Studies in Astronomy and Astrophysics
University of California at Santa Cruz
Santa Cruz CA 95064

and

Lawrence Livermore National Laboratory
Livermore CA 94550

Thomas A. Weaver+

Lawrence Livermore National Laboratory
Livermore CA 94550

* Work supported in part by the National Science Foundation under contract AST-79-09102

+ Work performed under the auspices of the U. S. Department of Energy under contract number W-7405-ENG-48.

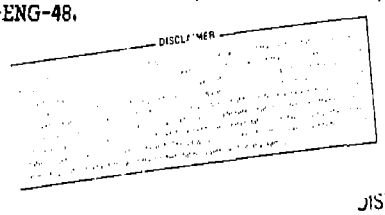

INTRODUCTION

Supernovae, because of their enormous energy impulse, ability to create heavy elements, form neutron stars and black holes, and due to their association with stellar death, have long played a central role in our models of the cosmos. Yet, after decades of study, our theoretical understanding of such events remains rather primitive. Our difficulties stem in part from the incomplete nature of the observational sample. No pre-supernova star has ever been identified[1] and detailed information on the complete evolution of all but a few supernovae is sadly lacking. There is also considerable diversity in the observed phenomena we are to explain. "Supernovae" include, in addition to the fairly regular class (or two subclasses[2,3]) of Type I supernovae, a wide variety of Type II supernovae[4], subluminous, slow supernovae[5] sometimes classified Type V, the progenitor of CAS A (apparently 4 magnitudes dimmer[6] than a typical Type II), and the Crab Nebula progenitor[7]. To these one may also need to add optically "invisible" supernovae, in which an accreting white dwarf occasionally collapses to a neutron star with little in the way of mass ejection or electromagnetic display[8], and, perhaps, an early generation of very massive ($M > 100\ M_\odot$) stars for nucleosynthesis. Theoretical models for supernovae are similarly diverse and probably more than one mechanism is required to explain all occurrences. Currently fashionable models include iron core collapse accompanied by hydrodynamical bounce at nuclear density (as discussed by Bethe in the preceding paper), thermonuclear detonation of white dwarfs and degenerate stellar cores[9,10], the pair instability in very massive stars[11], pulsar driven mass ejection[12], and various other magnetohydrodynamical phenomena[13-18]. A proper study of core collapse in massive stars might also need to include such multi-dimensional effects as rotation[19-22], magnetic

fields[13-18], and convective core overturn[23-26].

At the last Texas Symposium Weaver and Woosley[27] presented results for the complete evolution of massive stars and their explosion as Type II supernovae. These results, in good accord with the observed properties of such explosions, were predicated upon the assumption that core collapse in a massive star is capable of generating a strong, mass-ejecting shock wave. The intervening 2 years have not brought a definitive resolution to the core bounce problem although, as discussed by Bethe, there appears to be no fundamental obstacle standing in the way of such an occurence.

In this paper we will review recent progress, especially by ourselves and Axelrod at Livermore, in understanding the observed properties of Type I supernovae as a consequence of the thermonuclear detonation of white dwarf stars and the ensuing decay of the ^{56}Ni produced therein[28-30]. We shall also present, within the context of this model for Type I explosions and our 1978 model for Type II explosions, the expected nucleosynthesis and gamma-line spectra[31] from both kinds of supernovae. Finally we will discuss a qualitatively new approach to the problem of massive star death and Type II supernovae based upon a combination of rotation and thermonuclear burning. Preliminary studies by Bodenheimer and Woosley[32] (see also ref. 20) have shown that it may be possible to produce many of the observed properties of such supernovae even in situations where the collapse of the iron core in a massive star does not lead to a strong, mass-ejecting shock wave.

TYPE I SUPERNOVAE

A. Models

Observational constraints lead us to consider certain classes of stars as likely Type I supernova progenitors. In view of the non-correlation of Type I events with the location of galactic spiral arms[33], one should consider stars of relatively low mass. In particular, stars of greater than about 10 $M_\odot$, which have main sequence lifetimes shorter than 25 million years, seem unlikely candidates. Such a notion is reinforced by other theoretical considerations. Ten solar masses is a transition region from degenerate to non-degenerate core evolution. Stars heavier than about 10 $M_\odot$ will end their lives undergoing a core collapse[27,29,34,35] and, depending on the strength of the explosion, will leave behind a neutron star or black hole remnant. The degenerate nature of lower mass stars makes them more prone to thermonuclear instabilities and disruption, often leading to the production of a large amount of radioactive elements. The absence of hydrogen lines in the spectrum of Type I supernovae, lack of a well defined plateau phase in the light curve (a phenomena generally attributed to a transparency wave from hydrogen recombination "eating its way" into an extended red giant atmosphere[27]), and higher photospheric velocity all argue strongly for Type I candidate stars that lack a hydrogen envelope. Thus if massive stars are to produce Type I supernovae they must shed their hydrogen envelopes, either by a stellar wind or mass exchange in a binary system prior to exploding and, at the same time, retain a core mass in excess of the Chandrasekhar value.

This restriction may pose difficulties for Type I models involving intermediate mass stars lighter than about $8M_\odot$. Unless such stars lose their hydrogen envelope

prior to the second convective dredge-up phase[36], they will evolve into a configuration in which a thin, thermally unstable helium shell surrounds a degenerate, low mass carbon-oxygen core[37]. Since the helium shell in such stars contains only a few thousandths of a solar mass, growth of the core can proceed only by processing hydrogen envelope material through the helium shell (although in a complicated fashion[37]). Only two possibilities exist for the final evolutionary state. Either the repeated helium shell flashes are ultimately successful in completely ejecting the hydrogen envelope[38] before the core achieves the Chandrasekhar mass, in which case a white dwarf and planetary nebula result, or else the core eventually grows to critical mass and explodes while still retaining a portion of its hydrogen envelope. The latter case produces a Type II, but not a Type I, supernova. Restrictions of this kind can be circumvented for intermediate mass stars heavier than about 6 $M_\odot$ if the hydrogen envelope is removed prior to the second convective dredge-up phase. In that case a helium core mass larger than the Chandrasekhar value is left behind[36] and the thin helium shell phase is never achieved. These arguments also clearly do not apply to white dwarf stars accreting mass in binary systems, except possibly in the case of very high accretion rates[39].

Such considerations have led researchers interested in studying Type I supernovae to concentrate their efforts on two general classes of models: 1) accreting white dwarfs and 2) the final evolutionary stages of single stars that have main sequence masses in the range 7 $M_\odot$ to 10 $M_\odot$. In this latter case the star is presumed to have lost its hydrogen envelope (which comprises roughly 80% of its main sequence mass) prior to the explosion of the core, and ends its life as a bare helium-surfaced core of roughly 1.5 $M_\odot$ to 2.5 $M_\odot$. It is noteworthy in this regard that a 9 $M_\odot$ star will spend almost 4 million years as a red supergiant star[28] having a radius slightly greater than 1 AU. Thus an average mass loss rate of 2×10^{-6} $M_\odot$/yr, which is in the

range of observation[40], could remove the hydrogen envelope of such a star leaving a remnant of around 1.6 $M_\odot$. This assumes, as seems plausible, that the loss of the hydrogen envelope does not grossly affect the core evolution. Having lost its envelope, the stellar core may evolve to an unstable configuration and explode either due to a hydrodynamical bounce[29,34,35,41-43] or, perhaps, a thermonuclear instability[28,42].

In order to have a specific model to illustrate recent calculations of Type I supernova properties we will discuss a thermonuclear scenario based upon an accreting white dwarf. As we shall see critical observational results do not seem to be overly sensitive to many characteristics of the particular model employed. This is reassuring given the uniformity of Type I supernovae as a class. Accreting white dwarf models have been considered in many theoretical investigations[28,29,41,42,44-52]. The particular white dwarf model we wish to consider here in greatest detail results from a 0.5 $M_\odot$ C/O white dwarf accreting matter from a companion star at a rate 1.0×10^{-8} $M_\odot$/yr and has been studied by ourselves and Taam[28,29,50,51]. Similar behavior is expected[42,50,51] for a variety of C/O core masses and accretion rates in the range roughly 5×10^{-10} to 3×10^{-8} $M_\odot$/yr. For still lower accretion rates a central carbon detonation may occur[42]. In this particular model the hydrogen shell flashes should be weak so that, unlike a nova, most of the accreted matter stays on the white dwarf[50]. After 0.62 $M_\odot$ of helium has accumulated on top of the carbon-oxygen core, ignition occurs at the helium-core interface. Note that the white dwarf has not reached the Chandrasekhar mass in this case. Ignition is due to a combination of high density (accompanied by enhanced nuclear screening) and gravitational heating by compression from the growing layer of helium. The subsequent evolution is shown in FIGURE 1. A thermonuclear runaway begins at the base of the very degenerate helium shell. The local overpressure generated by this runaway (about a factor of 5) is sufficient to

initiate a pair of detonation waves, one propogating in through the carbon-oxygen core, the other out through the helium layer. Within 0.20 seconds the entire white dwarf, except for a few thousandths of a solar mass of helium on its surface, is incinerated into a nuclear statistical equilibrium dominated by ^{56}Ni and 2.4×10^{51} erg of energy is released. This is more than enough energy to entirely disrupt the star (which had an initial binding energy of 2.2×10^{50} erg) with a mean terminal velocity of 14,000 km/sec (see FIGURE 1d). The exploding material is accelerated partly by the detonation associated shock waves, but principally by adiabatic expansion. In the steep density gradient at the surface very high velocities are attained by shock wave acceleration and a small, uncertain fraction of mass (we estimate less than 10^{-9} $M_\odot$) is accelerated to relativistic velocities. As the ejecta expand and cool rapidly, the reactions maintaining the nuclear equilibrium "freeze-out" yielding a final composition (FIGURE 2) dominated by ^{56}Ni. Due to the rapid quenching of the equilibrium about 6% by mass of helium is also ejected along with the iron group[29,53].

B. Light Curve

The subsequent observable behavior of the detonated dwarf described above has been calculated by Weaver, Axelrod, and Woosley[28]. Within the roughly 10 seconds it takes the dwarf to expand to several times its initial radius it has reached a homologous configuration which, barring outside interaction or growth of 2 and 3 dimensional instabilities, it will maintain indefinitely. In this configuration the velocity of a given mass element remains constant in time. At early times the entire supernova is opaque and, as a result, almost all the energy of the explosion is converted into kinetic energy of expansion. Very little energy escapes in the form of

light except for a brief, but intense, flash of hard radiation as the shock wave breaks out of the dwarf surface. (We are unable to properly calculate the characteristics of this flash without special relativistic modifications to our hydrodynamical code.) It follows that, except for the first few moments of their existence, the observable properties of such Type I supernova models will be determined solely by their final composition and Lagrangian profiles of velocity and density (which are related since r(m)=v(m)t). Most thermonuclear models employ near relativistic white dwarfs of similar density structure (ie. n=3 polytropes) as starting points, either as "bare" white dwarfs in cataclysmic variable systems or as the cores of more massive stars. Also the degenerate nature of the nuclear burning implies that the bulk of the explosive energy impulse is deposited in a time that is short compared to that required for the white dwarf to expand to several times its initial radius. It follows that the chief distinguishing properties of the models will be determined by: 1) the mass of the white dwarf core (which specifies, among other things, its specific gravitational binding energy), 2) the fraction of the star that burns to radioactive ^{56}Ni and the energy deposition from that burning (ie. its initial composition), and 3) for the cores of 7-10 $M_\odot$ stars, the properties of the overlying helium shell that can decelerate the expansion of an exploding white dwarf. Since a variety of physically plausible models can be constructed that give similar values for these parameters, it is not too surprising that a given set of observations may have more than one successful physical model.

An interesting check on this hypothesis has been performed by Weaver, Axelrod, and Woosley[28] who studied the light curves resulting from a variety of thermonuclear models. One study consisted of repeating the above exploding white dwarf calculation but bypassing the expensive computation of dual detonation waves by simply depositing instantaneously the amount of energy per gram obtained by complete combustion of the

initial composition to ^{56}Ni. Except in the surface layers, where shock wave steepening is important, the observable properties of the two models were identical. In the same study a similarly parametrized set of calculations were carried out for a variety of white dwarf masses as well as the "helium-tamped" core explosions of 9 and 10 $M_\odot$ stars (whose white dwarf cores are surrounded by a few tenths of a solar mass of low-density helium). The resulting velocity profiles at a late time when the stars coast in a homologous configuration are shown in FIGURE 3. Note the similarity of these profiles, both in magnitude and shape, for initial models of considerable diversity.

Since the bulk of the explosion energy goes into expansion (all but about 10^{45} erg in the model considered) one must look elsewhere for an energy source to explain the light output from a Type I supernova. That source, as first hypothesized by Burst[54] and studied for the nucleus ^{56}Ni by Pankey[55] and (independently by) Colgate and McKee[56], is radioactivity. Considerable success has been achieved in recent years in employing the radioactive model to interpret the light curve and spectrum of Type I supernovae[28,30,43,48,49,57,58]. The basic results may be summarized as follows.

The weak decay of ^{56}Ni to ^{56}Co (τ_{Ni} = 8.80 days) and of ^{56}Co to ^{56}Fe (τ_{Co} = 113.7 days) leads to a net nuclear energy deposition rate of

$$\dot{S}(t) = 3.90 \times 10^{10} \exp(-t/\tau_{Ni}) + 7.03 \times 10^{9} [\exp(-t/\tau_{Co}) - \exp(-t/\tau_{Ni})] \text{ erg g}^{-1}\text{ s}^{-1} \quad (1)$$

The cobalt decay is special, as pointed out by Arnett[43], in that 4% of the total deacay energy resides in the kinetic energy of the positrons. This energy will be deposited locally long after the expanding supernova becomes transparent to gamma-radiation. As Axelrod[30] has pointed out even a microgauss magnetic field suffices to confine the positron to the immediate vicinity of its origin. The

luminosity of a Type I supernova is then given by[28]

$$L(t) = M_{56}\,\dot{S}(t-\tau_1)\,f_{dep}(t-\tau_1)\,f_{esc}(t)\ \text{erg s}^{-1} \qquad (2)$$

where M_{56} is the mass of radioactive ^{56}Ni produced by the explosion, f_{dep} is the (time dependent) fraction of the nuclear decay energy deposited locally (a lower bound being 0.04 as discussed above), f_{esc} is the (time dependent) fraction of deposited energy that avoids adiabatic decompression to escape as optical (or near optical) radiation, and τ_1 is the mean time between energy deposition and escape (or decompression). Weaver, Axelrod, and Woosley[28] have given analytic expressions that allow the simple calculation of the energy deposition and escape factors for a variety of supernova models. FIGURE 4 shows these for the exemplary model we have been discussing. As might be expected, these functions depend sensitively upon the initial density profile as well as the final velocity profile and opacity of the expanding material. We will note here just the general behavior. Initially $f_{esc} = 0$ and $f_{dep} = 1$, that is all radioactive energy is deposited but none is able to escape because the supernova is still completely optically thick. After a period of about 10 days the photospheric radius begins, for a reasonable choice of opacities, to recede in Lagrangian coordinate into the expanding supernova (see FIGURE 5) as the radiative diffusion time scale (for optical light) becomes comparable to the expansion time scale. As a result the energy escape factor is rapidly increasing at a time about 10 days after explosion while the energy deposition factor stays near unity. Since the maximum possible luminosity is generated at the earliest time that the supernova becomes transparent this is also the time of maximum optical light output. Past this point the light output becomes less sensitive to the escape fraction, which asymptotically approaches unity, and more to the energy deposition parameter which

slowly deceases from unity as the region of gamma transparency progresses inward in Lagrangaian coordinate. The progression of this transparency wave is sensitive to the adopted density and velocity profiles and will be slowest in the central regions of the star. For the model we have been describing f_{dep} falls to 0.5 after 35 days and to 0.1 after 110 days. During this period the luminosity declines considerably faster than would be expected solely from the simple time dependence of eq(1). After about 2 years the entire supernova has become essentially transparent to the gamma-rays from nuclear decay and pair annihilation (but not to the positrons themselves) and the (bolometric) luminosity is given to good accuracy by eq (1) with $f_{dep} = 0.04$ and $f_{esc} = 1.0$. At very late times the decay of ^{44}Ti may also contribute positrons and kinetic energy input[29], but this was not included in the present calculation.

An interesting complication to the optical luminosity of Type I supernovae has been discussed by Axelrod[30] who predicts a qualitative change in the wavelength of principal emission around 2 years after the explosion. At that time emission is coming chiefly from collisionally excited lines of Fe II and Fe III. The cooling curves for these ions have an interesting property which reflects the paucity of strong, collisionally excited transitions for wavelengths between about 10 microns and the optical band. For low emissivity the energy radiated by such an ionized iron plasma is almost entirely due to collisionally excited infrared transitions, but for higher emissivity an increasingly large fraction of the flux comes out in the form of optically visible lines. Thus early on in a Type I supernova, when the energy flux is quite large, the great bulk of the emission will be in the optical band. Later however, as the energy input by radioactivity diminishes exponentially, there comes a time when infrared transitions can, and do carry most of the luminosity. The nature of the cooling curves of Fe II and Fe III is such that this qualitative change in the spectrum occurs rather suddenly (for an assumed constant density). Thus Axelrod has

termed this occurence the "infrared catastrophe" meaning that, below a certain critical flux, the optical output of a Type I supernova will be catastrophically diminishd and most emission will instead be in the infrared (especialy in the waveband 20 to 100 microns). This infrared emission, about 10^{39} erg/sec at 2 years would in principle, be observable from supernovae in the Virgo cluster by a satellite experiment such as the planned Space Infrared Telescope Facility (SIRTF) or, for the shorter wavelengths, by a ground-based 10 meter telescope. It has not and should not have been observed thus far due to its onset at very late times (when the supernova luminosity has declined considerably) and the long wavelength of its characteristic emission (20 to 100 microns). For an expanding iron sphere of assumed constant density Axelrod[30] finds at an age of 400 days, an infrared emission that is only about 1% that of the optical and at 850 days, 10%. In a more realistic model containing a density gradient the onset of this "infrared catastrope", which occurs first in the dense core where the electron collision rate is higher and later in the rest of the star, is delayed and spread out over a longer time period. Its observational impact is correspondingly diluted.

The actual light curve determined for our standard model[28] is shown in FIGURE 6. The late time behavior was calculated using the photonics transport code (multi-group, multi-angle) of Axelrod[30] and excludes energy emitted in the infrared. The slight change in slope at around 600 to 700 days is a result of this subtraction and is a measure of the "infrared catastrophe" in this particular model. Similar light curves have been obtained for other detonating white dwarfs and 8-10 $M_\odot$ cores[28]. Based upon the light curve for SN 1972e Axelrod has also determined an allowable range of ^{56}Ni masses. Assuming that NGC 5253 is located 2 to 4 Mpc from the earth the requisite amount of radioactive nickel is 0.4 to 1.4 $M_\odot$. This requirement strains, but does not rule out hydrodynamical bounce models such as the one discussed by Arnett[43] which,

because they retain most of their high density matter in a collapsed remnant, have difficulty ejecting even a few tenths of a solar mass of iron-group elements. This range of nickel production is quite natural for thermonuclear disruptions and is an argument, although not yet overwhelming, in their favor.

C. The Spectrum and Evidence For Radioactive Cobalt In Type I Supernovae

Considerable progress, both observationally and theoretically, has recently been achieved in the study of Type I spectra. This is especially so within the context of the radioactive model at late times[28,30,57-60]. At early times, particularly near and just following maximum light when many observers like to do their work, the spectrum may be exceedingly complex and difficult to interpret. This is because, as was discussed in the previous section, maximum light is achieved just as the supernova is becoming transparent to its own light (see FIGURES 4, 5, and 6). Emission from the photosphere at this time is likely to be modified both by absorption and by the extensive, non-LTE emission of lines powered by radioactive input from ^{56}Ni and ^{56}Co in the region above the photosphere.

Branch[61,62] and coworkers[63] have recently studied the spectrum of Type I supernova 1972e at a time about 25 days following its explosion in an attempt to place constraints on the composition of the ejected outer layers. Using a synthetic spectrum composed of P-Cygni absorption line profiles superimposed upon a well defined continuum, he finds evidence for dominant line features from resonant scattering by Ca II, Si II, Fe II, and He I. Spectra from a number of other Type I explosions seem to exhibit similar features emphasising the homogeneity of this class of supernovae. However, the tentative conclusion by Branch[61,62] that these early time spectra show evidence for an enhanced iron, but not enhanced cobalt abundance in a region (just

above the photosphere) having velocity greater than 80.0 km/sec, cannot be reconciled with the model we have been discussing (which would have about 4 times as much cobalt as iron at this time) or, for that matter, with any (presently known) uncontrived model. Hopefully this constraint will be relaxed with better atomic data and with a more careful and complete treatment of non-LTE processes at early times. It is to be emphasized in this regard that if the spectrum of SN 1972e at 25 days in fact contains, in addition to the assumed continuum and absorption lines, broad emission line features such as are predicted by the radioactive model[28,30,57,58] and seen in the late time spectrum[60], the abundance constraints of Branch might well be in error.

Branch has also observed in the early time spectrum of SN 1972e calcium absorption features that imply an upper velocity limit in the overlying ejecta of less than about 13,000 km/sec, considerably less than in our 'standard' model (see FIGURES 2 and 3) which has substantial amounts of freshly synthesized calcium in the outer layers moving with velocities greater than 30,000 km/sec. This constraint, which depends only upon measuring a Doppler width for a strong absorption line, is probably a stringent one. It suggests that the particular "deflagration" model we have been considering is probably too energetic to have been the exact progenitor of SN 1972e, a conclusion that we will find reinforced by other spectral considerations at late times. The other, less energetic white dwarf models[28] whose velocity profiles were shown in FIGURE 3 would be in better accord with these constraints.

The late-time spectra of Type I supernovae, while apparently not a result of emission from a plasma in local thermodynamic equilibrium, are somewhat simpler to model than at earlier epochs when a photosphere exists. Kirshner and Oke[60] first pointed out the resemblence of certain features in the late optical spectrum of SN 1972e to those produced by a blend of lines of Fe II and III. Subsequent examinations by Meyerott[57,58] and, especially, Axelrod[30] have elucidated the atomic mechanisms

whereby the gamma-rays and positron kinetic energy from nuclear decay are converted into optical emission. These decay particles expend most of their energy ionizing the plasma (in the case of gammas via intermediary suprathermal electrons produced by Compton scattering) and in heating the electron gas. Recombination produces ultraviolet radiation which ionizes still more atoms producing a bath of thermal electrons that is augmented by the Auger electrons from higher excitations. The ultraviolet line opacity here is much greater than the optical line opacity. A steady state is achieved in which recombination balances ionization and this balance determines the dominant ionization stages. Similarly, heating is balanced in steady state by radiative cooling from excitations produced by collisions with the thermal electrons. Continuous emission is negligible. As time passes and the supernova expands, the electron number density, n_e, (to which the recombination rate is proportional) will decrease but then so will the ionization energy input per particle from radioactive decay [eq(1)]. The ionization state is most sensitive to the ratio $S(t)/n_e$ which at late times scales[28] as $t^3\exp(-t/\tau_{Co})$, a function that varies only slowly with time during the interval 150 days to 600 days. This explains why the same ionization stages are prevelant over such a long period of observation. It also explains, qualitatively, why after about 2 years Axelrod[30] finds an increase in the relative efficiency of infrared emission (see the previous section). It is at that time that the energy input per particle from nuclear decay finally begins to decrease relative to the (collisionally excited) emission per particle.

The optical spectrum resulting from our standard detonation model[28] at an age of 255 days is shown in FIGURE 7 compared to that observed from 1972e at the same age. This calculation used Axelrod's[30] spectral synthesis code in a coarsely zoned (6 mass elements) model to incorporate properly the presence of density and velocity gradients. The results of the model are in good agreement with the observed spectrum

of SN 1972e even though this model was not constructed to be representative of that particular object. Excesses of lines from high ionization stages of iron (eg. Fe V and Fe VI) confirm the suspicion suggested by the early time spectrum that this particular model was somewhat too energetic, ie. reached too low a density at too early a time (thus increasing the ratio $\dot{S}(t)/n_e$), to have been the exact progenitor of SN 1972e. More massive white dwarfs and/or white dwarfs whose explosions were characterized by lower specific energy deposition or capped with layers of helium would probably have spectra that are more consistent with SN 1972e[28].

Also seen in the spectrum of the theoretical model and in that observed for SN 1972e on Julian date 2441684 is a line feature due to a blend of lines from Co III at a wavelength of about 6000 Å. This spectral feature demonstrates the presence of freshly synthesized, radioactive cobalt in SN 1972e, a most important result that is relatively insensitive to the specific stellar model employed. Axelrod[30] has found similar spectral features for a variety of parametrized Type I explosions (see FIGURE 8 for a representative example) provided only that the expansion velocity of the explosion is not too dissimilar from that actually observed for Type I supernovae. This deserves emphasis. The good fit to the spectrum shown in FIGURE 8 results, not from an artificial attempt to fit the spectrum by varying temperature, composition, and ionization stages, but purely from assuming a mass of ^{56}Ni and an expansion velocity. The ratio of iron and cobalt abundances is exactly what would be there 264 days after the initial explosion (as best as can be determined in Axelrod's model, the "age" of SN 1972e on JD 2441684) and the temperature and ionization stages present in the spectrum are those determined from a detailed tracking of the atomic processes resulting from radioactive energy input [eq (1)]. Furthermore, a similar good fit to the spectrum is obtained for all the late time observations of Kirshner and Oke[60] and the cobalt feature, both in the theoretical model as well as in the observations,

decays away in strength (relative to nearby strong emission lines from iron) with a half-life approximately equal to that of radioactive ^{56}Co (see FIGURE 9). Finally the amount of radioactivity present is also that required to explain the Type I light curve. The combined weight of these arguments is compelling. Radioactivity has been discovered in SN 1972e and is the power source for the supernova light curve.

An additional prediction of the model is that Type I supernovae should be especially favorable objects for study with a gamma-ray telescope. The gamma-ray spectrum from our standard model[31] is shown in FIGURE 10. Such a signal would be visible to the broad-line gamma-ray spectroscopy experiment on the Gamma-Ray Observatory even if the supernova were located in the Virgo cluster of galaxies.

E. Nucleosynthesis

If the theories of Type I supernovae we have been describing have merit, then the chief nucleosynthetic product of such events is iron-group species plus ^{44}Ca (ref. 29). Although the detailed calculations have yet to be carried out, the isotopic composition of the ejected iron will probably be similar to that calculated for the exploding white dwarf at the core of the "carbon detonation" supernova model[53]. Assuming one Galactic Type I event roughly every 50 years[1] over the 10^{10} year lifetime of the Galaxy the cosmic mass fraction[64] of iron (1.0×10^{-3}) and ^{44}Ca (1.6×10^{-6}) would be approximately produced. Thus it may be that most of the iron in our Galaxy has been synthesized in Type I supernovae with only a relatively small contribution from Type IIs. This is particularly interesting in light of observations of old metal-deficient stars that indicate the oxygen abundance in our Galaxy arose at an earlier epoch than the iron abundance[65]. Since oxygen almost certainly is a product of

quite massive stars[27] ($M \gtrsim 20\ M_\odot$) this suggests a relative increase in the rate of formation of massive stars (compared to whatever class of stars it is that makes Type Is) early in the Galaxy. Such a possibility has been suggested on other grounds[66] and is indicated by other nucleosynthetic considerations[67].

TYPE II SUPERNOVA MODELS

Our understanding of Type II supernovae still awaits a proper calculation, with universally accepted physics, that yields a strong outwardly propogating shock wave from a hydrodynamical core bounce in a massive ($M \geq 10\ M_\odot$) star. Most theoretical endeavor in the area of Type II supernova modeling during the last 2 years has centered on resolving this problem, especially with a more physical treatment of the equation of state for very high density matter. The difficulty of this problem and its present status have been reviewed by Bethe in the previous talk. If one-dimensional calculations are ultimately successful in yielding a sufficiently energetic shock wave, then studies by Weaver and Woosley[27,68] have already shown that good agreement with observed light curves and velocity, radius, and temperature histories can be achieved, as well as nucleosynthesis that (for a $25\ M_\odot$ model) resembles a solar abundance pattern.

A. Nucleosynthesis and Gamma-Ray Astronomy

Since the last "Texas" meeting nucleosynthesis in a $25\ M_\odot$ supernova model has been studied in much greater detail. The complete evolution of the star examined by Weaver, Zimmerman, and Woosley[69] and Weaver and Woosley[27,68] using a 19 isotope nuclear reaction network has been "post-processed" using a 131 isotope network and the synthesis of all species from carbon to nickel determined[67]. The results are shown in FIGURE 11 compared to the solar abundance pattern. It seems that the cosmic abundances of many isotopes in this mass range can be accounted for if approximately one gram in

14 of the Galactic mass has experienced conditions similar to those that prevail during the evolution of a 25 $M_\odot$ star. The relatively deficient production of species between silicon and iron is a consequence of inadequate amounts of matter experiencing temperatures in the range required for explosive oxygen burning and indicates, not too surprisingly, that not all of the elements in this mass region were created in a star of unique mass. We expect this deficient production of intermediate mass species to be compensated for by stars more massive than 25 $M_\odot$. Whether this will require some skewness of the initial mass function in the early evolution of the Galaxy remains to be seen. The iron abundance ejected in this model is particularly sensitive to uncertain properties of the core bounce so it may be that such supernovae eject far less iron than shown in FIGURE 11 (although evidence for a radioactive tail[27] in some Type IIs shows that they must occasionally eject at least a little ^{56}Ni). As discussed previously it is possible, although perhaps not necessary, that Type I supernovae produce most of the iron in the Galaxy.

The gamma-line spectrum that results from the nucleosynthesis in this model[31] is shown in FIGURE 12. Due to the obscuring influence of the extended red giant envelope in Type IIs, the radioactive nuclei do not become visible (at least in our one-dimensional model) until about a year after the explosion. Thus Type I supernovae are much better candidates for gamma-ray spectroscopy in other galaxies. For example, the signal shown in FIGURE 12 would not be visible to the Gamma-Ray Observatory from an explosion in the Virgo cluster of galaxies.

E. Type II Models With Rotation and Nuclear Burning

The theoretical results described above are predicated upon the assumption of a successful core bounce calculation and the neglect of such two dimensional effects as

rotation and magnetic fields. Given the present and historical quandry of the core bounce models, one begins to wonder about other alternatives, in particular, the possibility that core collapse in a massive star does not always (if ever) lead to a strong, mass-ejecting shock wave. If so, one is left to consider a most intriguing problem, the continued evolution of a massive, highly evolved star, endowed with rotation and combustible nuclear fuel, whose core has collapsed. While it seems highly likely that one component in the final outcome of such an occurence will be a black hole, it is less clear whether or not the formation of this black hole will be accompanied by substantial mass ejection (due to rotation, magnetic fields, and/or nuclear burning) and whether the observable event might still be properly called a Type II supernova. It is good to keep in mind that the free fall time scale for the red giant photosphere is several months whereas the time scale for dynamic occurences in the core is much more rapid. Any instabilities that can develop probably will develop. It does not appear likely to us that a black hole can eat a rotating red supergiant whole without burping!

Bodenheimer and Woosley[32] have begun a preliminary assesment of the continued evolution of a rotating (non-magnetized), 25 $M_\odot$, completely evolved star whose core bounce has failed. The initial model is taken from the one-dimensional work of Weaver, Zimmerman, and Woosley[69] and followed with a two-dimensional explicit hydrodynamics code[70]. Only the inner 8 $M_\odot$ of the star is followed in the two-dimensional study. Equation of state information is taken from tables generated by the KEPLER code of Weaver, Zimerman, and Woosley. Unfortunately, due to the Courant time limitations on an explicitly differenced code, the Bodenheimer-Woosley study is presently unable to include the collapsed core (in which the dynamic timescale is less than one millisecond) and stellar mantle (timescale on the order of seconds) in the same calculation. Instead the center of the star is removed from the calculation out to a

radius of 1.5×10^8 cm and replaced by an inner boundry condition that pressure be some fraction (initially taken equal to 1/2) of that required for local support in hydrostatic equilibrium. Nuclear energy generation from oxygen burning is included in the calculation as are neutrino losses. In the initial model the inner 2 $M_\odot$ of material is taken to consist of inert fuel (in as far as nuclear energy generation goes) and the region 2 to 8 $M_\odot$ is presumed to be pure ^{16}O. This is a reasonably good approximation to the stellar evolutionary results[69], at least for purposes of nuclear energy generation.

The choice of angular momentum distribution in any calculation of this sort is both critical and highly uncertain. Bodenheimer and Woosley[32] chose a total angular momentum of 4.5×10^{51} erg sec, roughly equal to that of the inner 8 $M_\odot$ of a main sequence O-star (presuming such stars to be rigid rotators; a lower bound if they are not). This momentum is distributed in the initial configuration in such a way as to provide a constant ratio (0.12 for the particular case under discussion) of centrifugal acceleration to (the axial component of) gravitational acceleration. This prescription gives a distribution of specific angular momentum that increases gradually outwards. The magnitude of these terms is consistent with studies by Endal and Sofia[71] of angular momentum redistribution in a highly evolved 10 $M_\odot$ star. The ratio of total rotational energy to gravitational binding energy in the 5.5 $M_\odot$ of material included in the problem but outside the core was 13%, which is marginally stable on a secular time scale and quite stable on a dynamic time scale[72].

Subsequent evolution of this configuration was followed numerically and several imporatant stages of development noted. Initially the entire stellar mantle responds to the decreased core pressure on a sonic crossing time. A near spherical collapse results with growing collapse velocities (FIGURE 13, first 3 frames) accompanied by increasing core mass and angular momentum. After about 2 seconds rotational braking in

the equator combined with the inability of the (finitely pressurized) inner boundry to accept accreting matter at an arbitrarily fast rate leads to a stagnation of collapse flow, especially in the equator (FIGURE 13, frames 3 and 4). The density contours of the star at this point have a "lobed" structure showing the presence of a thick accretion disk. Continued evolution results in an enlargement of this thick disk which eventually grows to include most of the matter in the mantle. At a time of about 3 seconds into the evolution it was noted that the angular momentum in the inner core (inside the pressure boundry condition) had grown so large (greater than 10^{50} erg s) that a rotating n=3 polytrope having the mass of the core (about 2.3 $M_{\odot}$) at that time would have, with any reasonable choice of angular momentum distribution[73], an equatorial radius that would intrude on the inner boundry radius of the problem (1.5 x 10^{8} cm). The mutiplication factor on the inner boundry pressure was therefore slowly raised over a period of 2 seconds (the timescale for doubling the core angular momentum by accretion) from its initial value of 1/2 to unity. This acted to slow, but not to stop, the further growth of the core mass and angular momentum. During this phase the ratio of rotational energy to gravitational binding energy in the core never exceeded 0.14 and was therefore deemed secularly (as well as dynamically) stable to tri-axial deformation[72]. Continued evolution resulted in the development of a persistent velocity configuration (FIGURE 14) in which material would fall in at high velocity from a region along the rotational axis and out to about 60 degrees from that axis, undergo a centrifugal bounce at around 3 x 10^{8} cm accompanied by the explosive nuclear burning of oxygen at a temperature of about 3 to 4 billion degrees, and then move outwards at high velocity along the equatorial plane. After a period of about 15 seconds, during which time more than 10^{51} erg of energy had been produced by nuclear reactions alone (most of which was swallowed by the inner boundry condition), a large blob (about 0.5 $M_{\odot}$) of oxygen burning products was observed propogating outwards in

the equator with velocity around 5000 km/sec and a total, outwardly directed kinetic energy of more than 10^{50} erg. At this point the calculation was terminated both because the ejected blob was impinging on the outer boundry of the problem and because Courant limitations on the material falling down the polar axis at very high velocity were causing the code to take very small time steps.

While the preliminary nature of this calculation is to be stressed and considerable concern may rightfully be expressed about the rather artificial treatment of the inner boundry condition, the results suggest an entirely different scenario for the production of at least some Type II supernovae than the often discussed core bounce mechanism. A considerable portion of the 10^{50} erg carried by the equatorially ejected blob will probably be deposited in the red giant envelope overlying the mantle of the star. Since the blob will encounter roughly its own mass in traversing the envelope, deposition of this energy will likely lead to a shock wave propogating through the atmosphere which may, in time, forget its very asymmetric origin. It is this shock wave interacting with the envelope that is the cause of most of the optical display associated with Type II supernovae. Except perhaps for a somewhat lower total energy, the observable results from this model might be quite similar to those calculated for the core bounce mechanism in the same star[27,68]. The final fate of the star and its nucleosynthesis however would be quite different. The final residual would almost certainly not be a neutron star, but instead, a black hole (the mass of the inner core was already above 3.3 $M_\odot$ after 15 seconds of evolution which presumably was far from complete). Far more explosive oxygen burning products would be ejected than in the one-dimensional, shock-wave-based calculation and, since momentum must be conserved, these debris might not have a spherical distribution. These "knots" of oxygen ashes could also retain a higher velocity than imparted to the bulk of the hydrogen envelope.

This is quite interesting in light of recent observations. Lasker[74], for example, has studied a supernova remnant in the Large Magellanic Cloud (SNR N132D) in which an annulus of oxygen-rich knots is observed all moving outwrds from a point with a velocity of several thousand km/sec, maintaining a torroidal structure. These results may also be highly relevent for CAS A which also displays a distribution of fast moving, oxygen-rich knots with similar, annular asymmetry[75] and thus far has shown no evidence for the presence of a neutron star remnant. Perhaps CAS A instaed contains a black hole! A third supernova remnant (0540-69.3, also in the LMC) has also been recently reported[76] to display a ring of oxygen-rich knots similar to those reported by Lasker for N132D. Apparently this is a fairly common phenomenon.

Clearly further investigation of this category of Type II model is indicated. A much more credible result could be obtained if the core and mantle could be carried in the same calculation. This will require the development of an efficient, fully implicit 2D-hydro code containing sufficient physics to track matter at quite high densities and pressures. Alternatively, although not quite as appealing, a separate calculation could be done of the inner core evolution and coupled to a mantle calculation like that of Bodenheimer and Woosley. The preliminary work of Tohlin, Schombert, and Boss[21] is a useful step in that direction. A systematic study of other recent supernova remnants to search for two-dimensional asymmetry such as that observed N132D, CAS A, and 0540-69.3 might also be very interesting.

REFERENCES

1 TAMMANN, G.A. 1977. in Supernovae. ed. D.N. Schramm. (D. Reidel: Dordrecht) 95.

2 BARBON, R., F. CIATTI & L. ROSINO. 1973 Astron. and Astrophys. 25:241.

3 BARBON, R. 1980 in Proc of the Texas Workshop on Type I Supernovae. ed. J.C. Wheeler. (Univ. of Texas Press: Austin) 154.

4 BARBON, R., F. CIATTI & L. ROSINO. 1974. in Supernova and Supernova Remnants. ed. C.B. Cosmavici (D. Reidel: Dordrecht) 115.

5 ZWICKY, F. 1964. Astrophys. Jour. 139:514.

6 ASHENHURST, R. 1980. Jour. Hist Astron. 11:1.

7 WHEELER, J.C. 1981. Reports on Progress in Physics (in press).

8 NOMOTO, K., S. MIYAJI, K. YOKOI & D. SUGIMOTO 1979. IAU Coll., No. 53, White Dwarfs and Variable Degenerate Stars. ed. H.M. Van Horn and V. Weideman. p. 56.

9 HOYLE, F. & W.A. FOWLER. 1960. Astrophys. Jour. 132:565.

10 ARNETT, W.D. 1969. Astrophys. Spac. Sci. 5:180.

11 BARKAT, Z., G. RAKAVY & N. SACK. 1967. Phys. Rev. Lettr. 18:379.

12 BODENHEIMER, P. & J.P. OSTRIKER. 1974. Astrophys. Jour. 191:465.

13 LE BLANC, J.M. & J.R. WILSON. 1970. Astrophys. Jour. 161:541.

14 KUNDT, W. 1976. Nature. 26:673.

15 MEIER, D.L., R.I. EPSTEIN, W.D. ARNETT & D.N. SCHRAMM. 1976. Astrophys. Jour. 204:867.

[16] BISNOVATYI-KOGAN, G.S., Y.P. POPOV & A.A. SAMOCHIN. 1976. Astrophys. Space Sci. 41:287.

[17] BISNOVATYI-KOGAN, G.S. 1980. Ann. N.Y. Acad. Sci. 336:389.

[18] MULLER, E. & W. HILLEBRANDT. 1979. Astron. Astrophys. 80:147.

[19] HOYLE, F. 1946. M.N.R.A.S. 106:343.

[20] FOWLER, W.A. & F. HOYLE. 1964. Astrophys. Jour. Suppl. No. 91. 9:201.

[21] TOHLINE, J.E., J.M. SCHOMBERT & A.P. BOSS. 1981. Los Alamos Preprint LA80-2870 & Spac. Sci. Rev. (in press).

[22] MÜLLER, E., M. RÓŻYCZKA & W. HILLEBRANDT. 1980. Astron. Astrophys. 81:576.

[23] EPSTEIN, R. 1979. M.N.R.A.S. 188:305.

[24] BRUENN, S.W., R.J. BUCHLER & M. LIVIO. 1979. Astrophys. Jour. Lettr. 234:L183.

[25] COLGATE, S.A. & A.G. PETSCHEK. 1980. Astrophys. Jour. Lettr. 236:L115.

[26] LIVIO, M., J.R. BUCHLER & S.A. COLGATE. 1980. Astrophys Jour. Lettr. 238:L139.

[27] WEAVER, T.A. & S.E. WOOSLEY. 1980. Ann. N.Y. Acad. Sci. 336:335.

[28] WEAVER, T.A., T.S. AXELROD & S.E. WOOSLEY. 1980. in Proceedings of the Texas Workshop on Type I Supernovae. ed. J.C. Wheeler (University of Texas Press: Austin). 113.

[29] WOOSLEY, S.E., T.A. WEAVER & R.E. TAAM. 1980. Proceedings of the Texas Workshop on Type I Supernovae. ed. J.C. Wheeler (University of Texas Press: Austin). 96.

[30] AXELROD, T.S. 1980. Ph.D. Thesis. Lawrence Livermore Laboratory Preprint UCRL-52994. See also Proceedings of the Texas Workshop on Type I Supernovae. ed. J.C. Wheeler (University of Texas Press: Austin). 80.

[31] WOOSLEY S.E., T.S. AXELROD & T.A. WEAVER. 1981. Comm. Nucl Part. Phys. (in press).

[32] BODENHEIMER P. & S.E. WOOSLEY. 1980. Bull. Am. Astron. Soc. 12:833.

[33] MAZA, J. & S. VAN DEN BERGH. 1976. Astrophys. Jour. 204:519.

[34] WEAVER, T.A. & S.E. WOOSLEY. 1979. Bull Am. Astron Soc. 11:724

[35] NITTA , S., K. NOMOTO, F. YOKOI, & D. SUGIMOTO. 1980. Publ. Astron. Soc. Japan. 32:305.

[36] BECKER, S.A. & I. IBEN. 1979. Astrophys. Jour. 232:831.

[37] IBEN, I. 1975. Astrophys. Jour. 196:525.

[38] TUCHMAN, Y., N. SACK & Z. BARKAT. 1979. Astrophys. Jour. 234:217.

[39] PACZYNSKI, B. & A. Tytkow. 1978. Astrophys. Jour 222:604.

[40] CONTI, P.S. 1978. Ann. Rev. Astron. Astrophys. 16:371.

[41] NOMOTO, K. 1980. in Proceedings of the Austin Conf. on Type I Supernovae. ed. J.C. Wheeler (University of Texas Press: Austin) 164.

[42] NOMOTO, K. 1981. in IAU Symposium No. 93. Fundamental Problems in the Theory of Stellar Evolution. ed. D. Sugimoto, D.Q. Lamb, & D.N. Schramm.

[43] ARNETT, W.D. 1979. Astrophys. Jour. Lettr. 230:L37.

[44] WHEELER, J.C. & C. HANSEN. 1971. Astrophys. and Spac. Sci. 11:373.

[45] WHELAN, J. & I. IBEN. 1973. Astrophys. Jour. 186:1007.

[46] MAZUREK, T.J. 1975. Astrophys. Spac. Sci. 23:365.

[47] NOMOTO, K & D. SUGIMOTO. 1977. Publ. Astron. Soc. Japan. 29:765.

[48] COLGATE, S.A., A. PETSHECK & J.T. KRIESE. 1980. Astrophys. Jour. Lettr. 237:L81.

[49] CHEVALIER, R.A. 1980. Fund. of Cosmic Phys. (in press) and preprint (submitted to Astrophys. Jour.).

[50] TAAM, R.E. 1980. Astrophys. Jour. 237:142.

[51] TAAM, R.E. 1981. Astrophys. Jour. 242:749.

[52] CAREFIELD, S., J.W. TRURAN & W.M. SPARKS. 1981. preprint.

[53] ARNETT, W.D., J.W. TRURAN & S.E. WOOSLEY. 1971. Astrophys. Jour. 165:87.

[54] BORST, L.B. 1950. Phys. Rev. 78:867.

[55] PANKEY, T. 1962. Ph.D. Thesis Howard University. Diss. Abstr. 23:#4.

[56] COLGATE, S.A. & C. McKEE. 1969. Astrophys. Jour. 157:623.

[57] MEYEROTT, R.E. 1978. Astrophys. Jour. 221:975.

[58] MEYEROTT, R.E. 1980. in Proceedings of the Workshop on Atomic Physics and Spectroscop, for Supernova Spectra. ed. R.E. Meyerott and G.H. Gillespie. (AIP: New York).

[59] KIRSHNER, R.P., J.B. OKE, M.V. PENSTON & S. SEARLE. 1973. Astrophys. Jour. 185:303.

[60] KIRSHNER R.P. & J.B. OKE. 1975. Astrophys. Jour. 200:574.

[61] BRANCH, D. 1980. in Proceedings of the Workshop on Atomic Physics and Spectroscopy for Supernova Spectra. ed. R.E. Meyerott & G.H. Gillespe (AIP: New York).

[30] AXELROD, T.S. 1980. Ph.D. Thesis. Lawrence Livermore Laboratory Preprint UCRL-52994. See also Proceedings of the Texas Workshop on Type I Supernovae. ed. J.C. Wheeler (University of Texas Press: Austin). So.

[31] WOOSLEY, S.E., T.S. AXELROD & T.A. WEAVER. 1981. Comm. Nucl Part. Phys. (in press).

[32] BODENHEIMER P. & S.E. WOOSLEY. 1980. Bull. Am. Astron. Soc. 12:873.

[33] [illegible] & S. VAN DEN BERGH. 1976. Astrophys. Jour. 204:519.

[34] WEAVER, T.A. & S.E. WOOSLEY. 1979. Bull. Am. Astron. Soc. 11:724

[35] MITA[illegible], K. NOMOTO, K. YOKOI, & D. SUGIMOTO. 1980. Publ. Astron. Soc. Japan. 32:303.

[36] BECKER, S.A. & I. IBEN. 1979. Astrophys. Jour. 232:831.

[37] IBEN, I. 1975. Astrophys. Jour. 196:525.

[38] TYCHMAN, Y., N. SACK & Z. BARKAT. 1979. Astrophys. Jour. 234:217

[39] PACZYNSKI, B. & A. Tutkow. 1978. Astrophys. Jour. 222:604.

[40] CONTI, P.S. 1978. Ann. Rev. Astron. Astrophys. 16:371.

[41] NOMOTO, K. 1980. in Proceedings of the Austin Conf. on Type I Supernovae. ed. J.C. Wheeler (University of Texas Press: Austin) 164.

[42] NOMOTO, K. 1981. in IAU Symposium No. 93, Fundamental Problems in the Theory of Stellar Evolution. ed. D. Sugimoto, D.Q. Lamb, & D.N. Schramm.

[43] ARNETT, W.D. 1979. Astrophys. Jour. Lettr. 230:L37.

[44] WHEELER, J.C. & C. HANSEN. 1971. Astrophys. and Spac. Sci. 11:373.

[45] WHELAN, J. & I. IBEN. 1973. Astrophys. Jour. 186:1007.

[46] MAZUREK, T.J. 1973. Astrophys. Spac. Sci. 23:365.

[47] NOMOTO, K & D. SUGIMOTO. 1977. Publ. Astron. Soc. Japan. 29:765.

[48] COLGATE, S.A., A. PETSHECK & J.T. KRIESE. 1980. Astrophys. Jour. Letter. 237:L81.

[49] CHEVALIER, R.A. 1980. Fund. of Cosmic Phys. (in press) and preprint (submitted to Astrophys. Jour.).

[50] TAAM, R.E. 1980. Astrophys. Jour. 237:142.

[51] TAAM, R.E. 1981. Astrophys. Jour. 242:749.

[52] CHAFFEE, S., J.W. TRURAN & W.M. SPARKS. 1981. preprint.

[53] ARNETT, W.D., J.W. TRURAN & S.E. WOOSLEY. 1971. Astrophys. Jour. 165:87.

[54] BORST, L.B. 1950. Phys. Rev. 78:807.

[55] PANKEY, T. 1962. Ph.D. Thesis Howard University. Diss. Abstr. 23:#4.

[56] COLGATE, S.A. & C. McKEE. 1969. Astrophys. Jour. 157:623.

[57] MEYEROTT, R.E. 1978. Astrophys. Jour. 221:975.

[58] MEYEROTT, R.E. 1980. in Proceedings of the Workshop on Atomic Physics and Spectroscopy for Supernova Spectra. ed. R.E. Meyerott and G.H. Gillespie. (AIP: New York).

[59] KIRSHNER, R.P., J.B. OKE, M.V. PENSTON & S. SEARLE. 1973. Astrophys. Jour. 185:303.

[60] KIRSHNER R.P. & J.B. OKE. 1975. Astrophys. Jour. 200:574.

[61] BRANCH, D. 1980. in Proceedings of the Workshop on Atomic Physics and Spectroscopy for Supernova Spectra. ed. R.E. Meyerott & G.H. Gillespe (AIP: New York).

62 BRANCH, D. 1980. in Proceedings of the Texas Workshop on Type I Supernovae. ed. J.C. Wheeler (University of Texas Press: Austin). 66.

63 BRANCH, D., S. FALK, M. McCALL, P. RYBSKI, A. UOMOTO, B. WILLS & D. WILLS. 1980. preprint.

64 CAMERON, A.G.W. 1973. Spac. Sci. Rev. 15:121.

65 TINSLEY, B.M. 1977. Astrophys. Jour. 229:1046.

66 SILK, J. 1977. Astrophys. Jour. 211:638.

67 WOOSLEY, S.E. & T.A. WEAVER. 1981. in Essays On Nuclear Astrophysics. ed. C.A. Barnes, D.D. Clayton & D.N. Schramm (Cambridge University Press).

68 WEAVER, T.A. & S.E. WOOSLEY. 1980. in Proceedings of the Workshop on Atomic Physics and Spectroscopy for Supernova Spectra. ed. R.E. Meyerott & G.H. Gillespe (AIP: New York).

69 WEAVER, T.A., G.B. ZIMMERMAN & S.E. WOOSLEY. 1978. Astrophys. Jour. 225:1021

70 BLACK, D.C., & P. BODENHEIMER. 1975. Astrophys. Jour. 199:619.

71 ENDAL, A.S. & S. SOFIA. 1978. Astrophys. Jour. 220:279. and 1977 Phys. Rev. Lettr. 39:1429.

72 OSTRIKER, J.P. & P. BODENHEIMER. 1973. Astrophys. Jour. 180:171.

73 BODENHEIMER, P. & J.P. OSTRIKER. 1973. Astrophys. Jour. 180:159.

74 LASKER, B.M. 1980. Astrophys. Jour. 237:765.

75 MARKERT, T.H., C.R. CANIZARES, G.W. CLARK & P.F. WINKLER. 1981. Bull. Am. Astron. Soc. 12:799.

76 MATHEWSON, D.S., M.A. DOPITA, I.R. TUOHY & V.L. FORD. 1981. Astrophys. Jour. Lettr. 242:L73.

77 AUSTIN, R.R.D. 1972. IAU Cir. No. 2421.

FIGURE CAPTIONS

FIGURE 1. - Conditions in a detonating white dwarf[29] of total mass $1.12M_{\odot}$. Initial thermodynamic conditions and composition (a) are taken from Taam[50] at a time just prior to ignition at the base of the highly degenerate helium layer. Energy transport is initially by convection (b) but, as the runaway progresses, subsonic convection is unable to carry the enormous energy generated by nuclear reactions. Shock waves are initiated, both inwards and outwards (c). In each shock the temperature rises to about 6 billion degrees and helium fuel is burned to a distribution of elements dominated by ^{56}Ni. The entire star is disrupted with the final velocity profile shown in (d).

FIGURE 2. - Final abundancies ejected by the detonated white dwarf[29] shown in FIGURE 1 are plotted against interior mass in solar masses (upper frame) and against external mass in grams (lower frame). Immediately following the explosion most of the star is in the form of (radioactive) ^{56}Ni and other iron-group elements. About 6% by mass of the total star is ^{4}He. A thin shell of the products of incomplete silicon burning remains at $M(r) \approx 0.5M_{\odot}$ where a rarefaction, caused by the oppositely moving shocks that initiated there, resulted in an anomalously low explosion temperature. Details of nucleosynthesis resulting from explosive helium burning in the outer layers of the dwarf are shown expanded in the lower frame. Terminal velocity, in units of 10,000 km s^{-1}, is also given at the top of the figure.

FIGURE 3. - Final velocity profiles as a function of interior mass fraction for 5 different Type I supernova models (taken from Weaver, Axelrod, and Woosley[28]). Solid lines are for 3 "bare" white dwarf models of indicated mass and composition. The top line is for our "standard" model defined in FIGURES 1 and 2. The other two (lower) solid lines are for compositions of 50% ^{12}C and 50% ^{16}O and 100% ^{20}Ne respectively. The dashed lines result from exploding the cores of 9 $M_{\odot}$ and 10 $M_{\odot}$

FIGURE 3 (continued)

stars whose hydrogen envelopes have been removed. In each case vertical bars indicate composition discontinuities. The 9 $M_\odot$ core was presumed to consist initially of 1.34 $M_\odot$ of oxygen and neon capped by 0.29 $M_\odot$ of low density ^{4}He. The 10 $M_\odot$ core was composed of 1.41 $M_\odot$ of carbon and oxygen, 0.15 $M_\odot$ of neon, carbon, and oxygen, and 0.47 $M_\odot$ of low density ^{4}He. All curves were calculated by assuming the instantaneous burning to ^{56}Ni of either the entire star (solid lines) or all material up to the first composition discontinuity (dashed lines). Note the similarity in the results.

FIGURE 4. - Time dependence of the energy deposition factor, the energy escape factor, and the delay time for the standard model.[28] The supernova light curve will reflect the decay rate of radioactive nuclei as modulated by these factors [see eq. (1)].

FIGURE 5. - Photospheric radius as a function of time for the standard model (taken from Weaver, Axelrod, and Woosley[28]). The three different curves result from employing a reasonable range of (uncertain) opacities in the expanding material.

FIGURE 6. - Light curve from the standard model compared to observational data for Type I supernovae (taken from Weaver, Axelrod, and Woosley[28]). In figure (a) numerically calculated light curves from the model are compared for the total, visual-, and blue band optical luminosity as labeled. Crosses are unreddened, integrated spectral scans[59] of SN 1972e for an assumed distance of 3.1 Mpc and explosion on Julian Date 2441433. The "*" s represent equivalently normalized, pre-discovery, photographic observations of Austen[77] and the "V", an earlier upper limit by the same author. The composite, blue-band, Type I supernova light curve as compiled by Barbon et al[4] is is also shown normalized in magnitude and shifted in time so as to provide the best fit. In (b) the late-time optical light curve (without infrared contribution, see text) is compared to the unreddened integrated spectral scans of Kirshner and Oke[60] and Kirshner et al[59]. The curves labelled "γ" and "e^+" show the contribution to the total light curve from γ-rays and positrons respectively.

FIGURE 7. - Comparison of the calculated spectrum from the standard model 255 days after explosion to the unreddened, spectral scan of SN 1972e taken by Kirshner *et al*[59] on Julian Date 2441684 (taken from Weaver, Axelrod, and Woosley[28]). Positions of major emission and absorption features are indicated with arrows. The observational data was normalized in magnitude so as to provide the best least squares fit. This particular normalization would place SN 1972e at a distance of 2.2 Mpc.

FIGURE 8. - The spectrum of a homogeneous sphere, initially consisting of 0.7 $M_\odot$ of pure ^{56}Ni expanding with constant velocity 7000 km s^{-1}, is compared [30,31] at a time 264 days after the beginning of its expansion to that of SN 1972e[59] on Julian Day 2441684 assuming the explosion occurred at 3 Mpc. At this time the calculated composition is 10% ^{56}Co and 90% ^{56}Fe and the temperature, about 5100 K. The top figure shows the model spectrum with cobalt lines included, the bottom shows it without cobalt lines (*ie.* only iron).

FIGURE 9. - In a format similar to FIGURE 8 the time history of the spectrum of Axelrod's [30, 31] expanding iron-cobalt sphere is compared to that of SN 1972e. Note the decay of the cobalt feature (about 6000 Å) compared to other nearby, strong lines of iron.

FIGURE 10. - The gamma-line spectrum[31] (due here entirely to lines from ^{56}Co decay) resulting from our standard detonating model [28,29] for Type I supernovae is shown at the indicated time for an assumed distance of 1 Mpc. The lines are extensively broadened by the high velocity of expansion. Due to the lack of an obscuring hydrogen envelope this emission is visible at a much earlier time than from a typical Type II supernova (see FIGURE 12) and therefore constitutes a much stronger signal.

FIGURE 11. - Nucleosynthesis expected from a 25 $M_\odot$, Type II supernova [27,67,68] compared to solar [64] abundances. An explosion energy of 10^{51} erg and remnant mass of 1.48 $M_\odot$ have been assumed. Dashed lines indicate a range of a factor of two about a consistent average overproduction factor of about 14. Nuclei below sulfur appear to be produced in reasonable proportions to account for their present Galactic abundances but the relative deficiency of element production in the range S to Mn is indicative of substantial nucleosynthesis in stars heavier than 25 $M_\odot$. Apparent overproductions may be due to uncertainties in cross section (Na, ^{36}S) or natural abundance (^{40}Ar). Some underproductions (e.g. N, ^{13}C) will be made up for in lighter stars.

FIGURE 12. - The gamma line spectrum [31] (due here entirely to lines from ^{56}Co decay) of the 25 $M_\odot$, Type II supernova [27, 67, 68] whose abundances were shown in FIGURE 11. It is assumed that the distance to the supernova is 1 Mpc. These spectral lines are not visible at earlier times due to the obscuring influence of the red supergiant envelope and, as a result, the signal is correspondingly weaker than for Type Is. (see FIGURE 10). The lines are also much narrower due to the lower characteristic ejection velocities [27,68] of heavy elements in Type IIs.

FIGURE 13. - Density and velocity profiles from a two-dimensional study of a rotating 15 $M_\odot$ star whose core has collapsed (taken from Bodenheimer and Woosley [32]). In the upper left frame, logarithmic density contours (10 per decade) are given for the initial model. The outermost contour shown has a density of 10^5 g cm^{-3} and the innermost 2×10^7 g cm^{-3}. In each of the velocity plots (other 3 frames) an arrow of unit length, 1000 km s^{-1}, is displayed in the upper right hand corner and a solid dark line is plotted as the locus of oxygen mass fraction equal to 0.5. This line is the approximate boundry between burned and unburned nuclear fuel. Initially (upper 2 frames) the collapse of the mantle is nearly spherically symmetric, but after about 2 seconds (lower left) rotation begins to inhibit infall in the equatorial plane leading to the growth of a thick "accretion disk." Several seconds later (lower right) a vortex-like velocity field has developed in the thick disk.

FIGURE 14. - Continued evolution of a collapsing rotating stellar mantle.[32] Format and density contour lines are the same as in FIGURE 13. The density profiles (left frame) show, some 15 seconds into the evolution, that the polar regions have been essentially evacuated. The entire stellar mantle exists as a thick, lobed accretion disk. The vortex flow pattern seen in the last frame of FIGURE 13 has been replaced by a persistent velocity field structure (right frame) involving high velocity mass ejection in the equatorial plane. The large, outwardly moving blob of oxygen burning ashes on the right hand side of the figure contains about 0.5 $M_\odot$. Exterior to the region shown on these plots, and out to a distance of about 4 astronomical units, the red supergiant envelope of the pre-explosive star[69] still waits, unaware of these dynamic occurrences in its core.

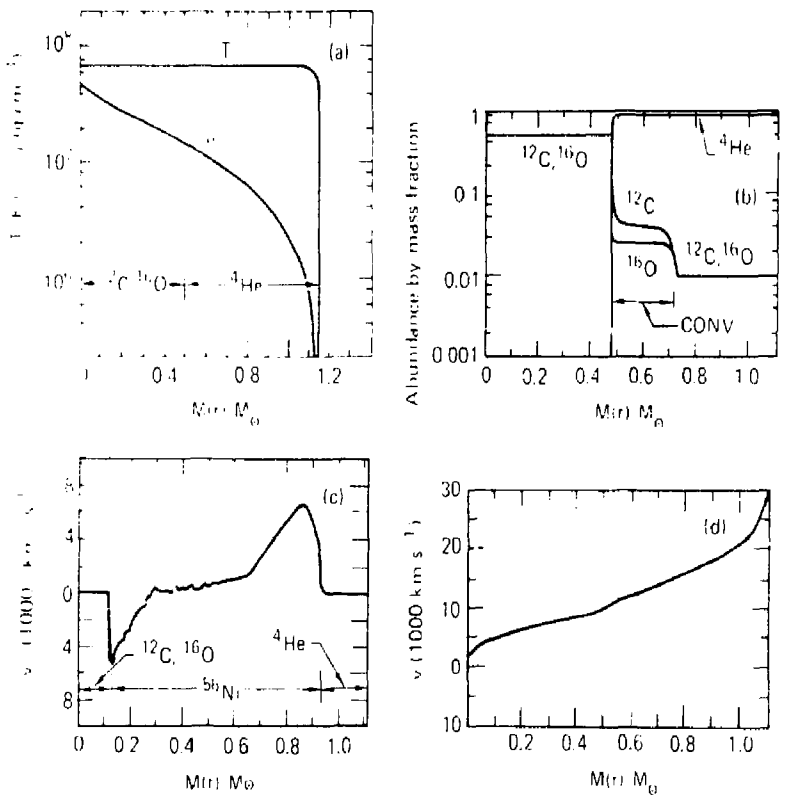
(a)
T
$^{12}C, ^{16}O$
^{4}He
0.4
0.8
1.2
M(r) $M_\odot$
(b)
$^{12}C, ^{16}O$
^{4}He
^{12}C
^{16}O
CONV
Abundance by mass fraction
1
0.1
0.01
0.001
0
0.2
0.4
0.6
0.8
1.0
M(r) $M_\odot$
(c)
$^{12}C, ^{16}O$
^{4}He
^{56}Ni
M(r) $M_\odot$
(d)
M(r) $M_\odot$

FIG. 1

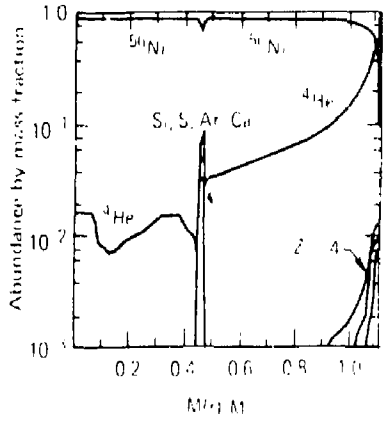
Abundance by mass fraction
1.0
10^{-1}
10^{-2}
10^{-3}
^{56}Ni
^{56}Ni
^{4}He
Si, S, Ar, Ca
^{4}He
Z
A
0.2
0.4
0.6
0.8
1.0
M/M

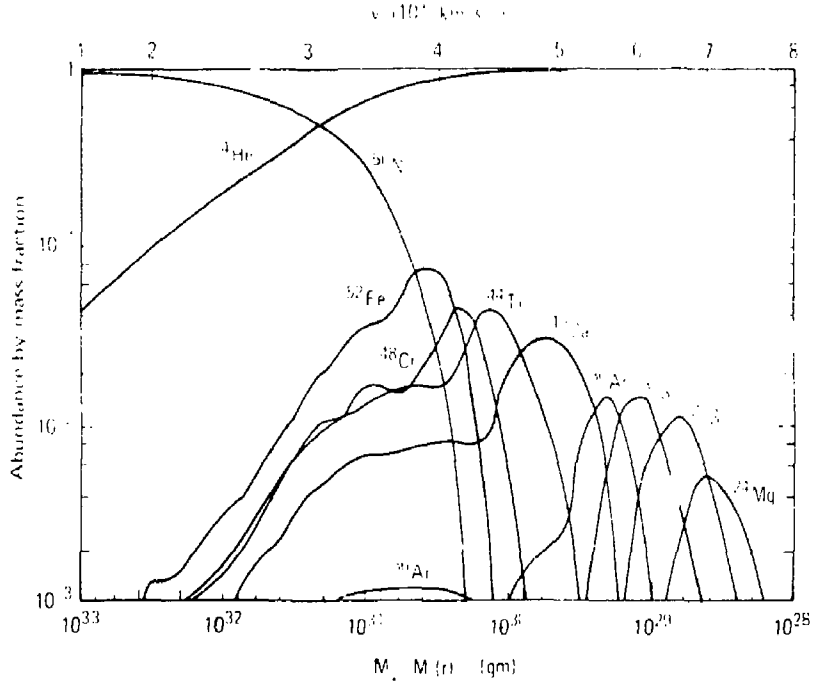
1
2
3
4
5
6
7
8
Abundance by mass fraction
1
10^{-1}
10^{-2}
10^{-3}
^{4}He
^{52}Fe
^{48}Cr
^{44}Ti
^{40}Ca
^{36}Ar
^{32}S
^{28}Si
^{24}Mg
^{20}Ne
^{16}O
^{12}C
^{8}Be
^{4}He
^{1}H
^{30}Ar
10^{33}
10^{32}
10^{31}
10^{30}
10^{29}
10^{28}
M, M (g) (gm)

FIG. 2

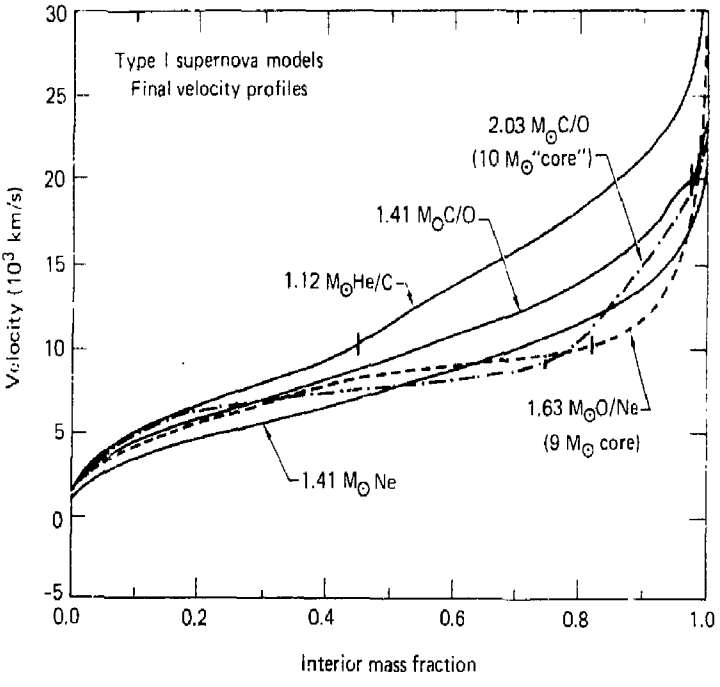
Type I supernova models
Final velocity profiles
2.03 M⊙C/O
(10 M⊙"core")
1.41 M⊙C/O
1.12 M⊙He/C
1.63 M⊙O/Ne
(9 M⊙ core)
1.41 M⊙ Ne
Velocity (10³ km/s)
Interior mass fraction
30
25
20
15
10
5
0
-5
0.0
0.2
0.4
0.6
0.8
1.0

FIG. 3

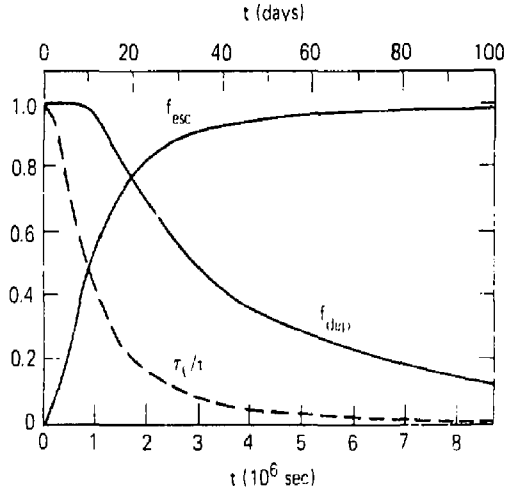
t (days)
0
20
40
60
80
100
1.0
0.8
0.6
0.4
0.2
0
f_{esc}
f_{det}
τ_i/τ
0
1
2
3
4
5
6
7
8
t (10^6 sec)

FIG. 4

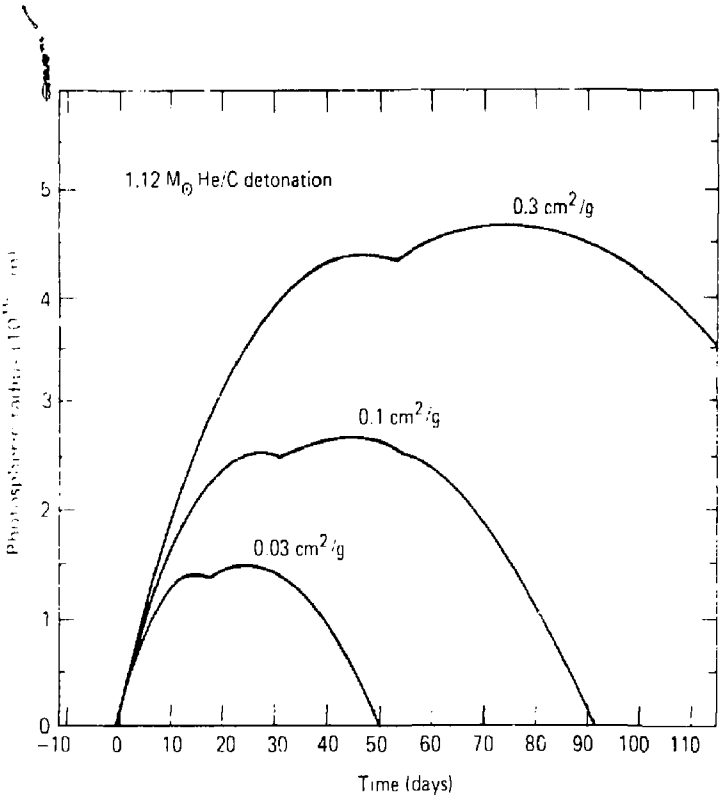
1.12 $M_\odot$ He/C detonation
0.3 cm^2/g
0.1 cm^2/g
0.03 cm^2/g
0
1
2
3
4
5
−10
0
10
20
30
40
50
60
70
80
90
100
110
Time (days)

FIG. 5

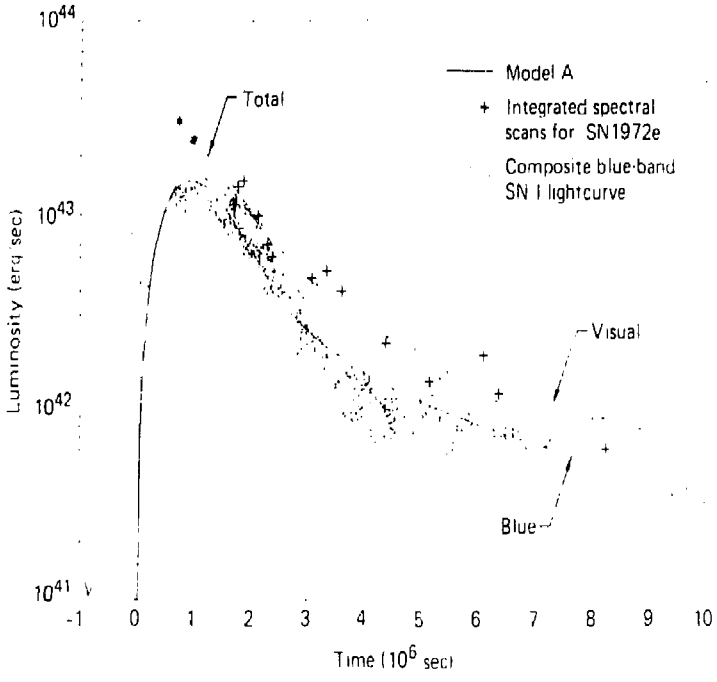
Model A
Integrated spectral scans for SN1972e
Composite blue-band SN I lightcurve
Total
Visual
Blue
Luminosity (erg/sec)
Time (10^6 sec)

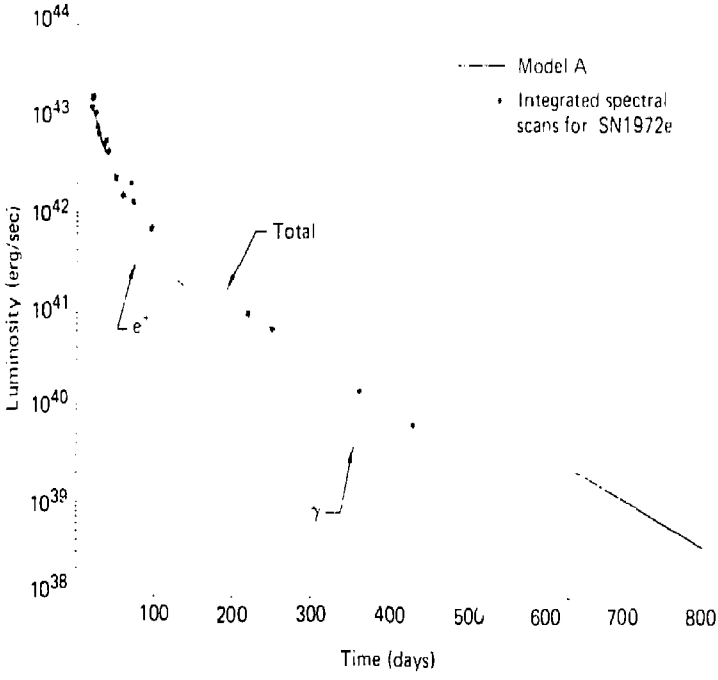
Model A
Integrated spectral scans for SN1972e
Total
e⁺
γ
Luminosity (erg/sec)
Time (days)

FIG. 6

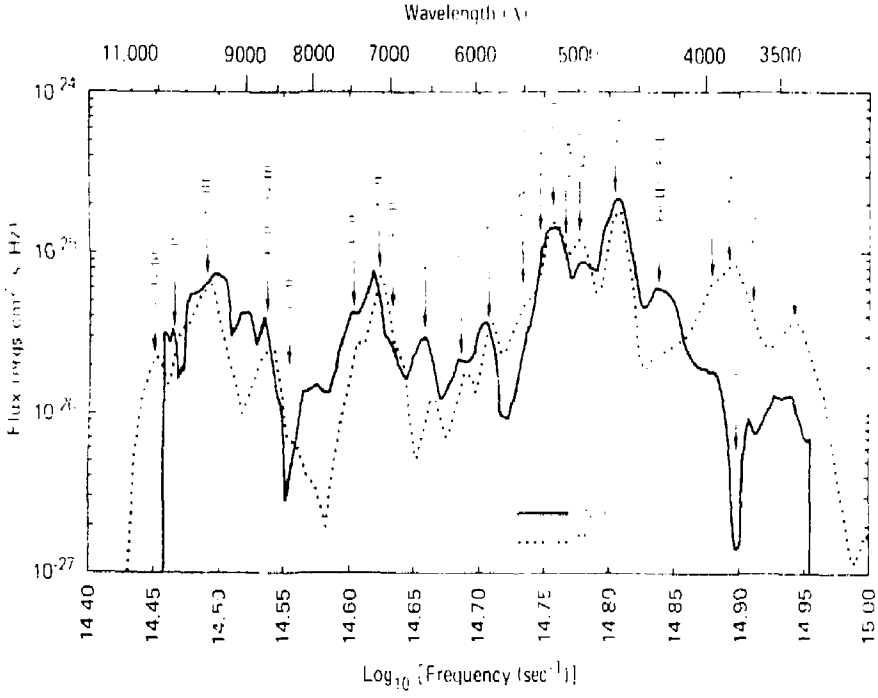
Wavelength (Å)
11,000
9000
8000
7000
6000
5000
4000
3500
10^{-24}
10^{-25}
10^{-26}
10^{-27}
14.40
14.45
14.50
14.55
14.60
14.65
14.70
14.75
14.80
14.85
14.90
14.95
15.00
$\log_{10}$ [Frequency (sec^{-1})]

FIG. 7

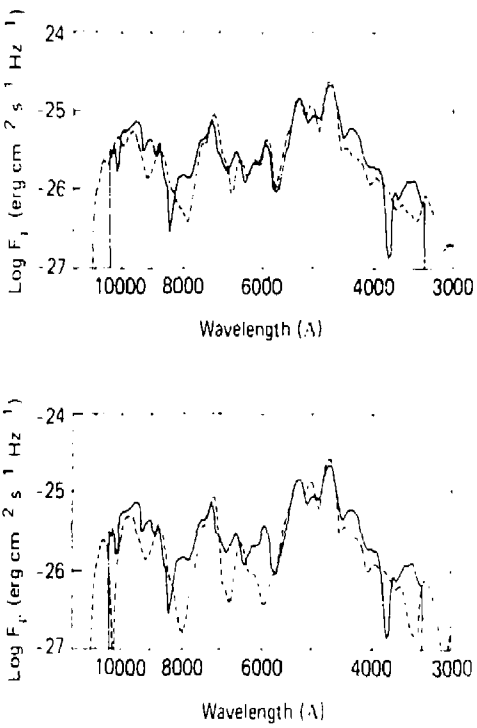
Log F_λ (erg cm $^{-2}$ s $^{-1}$ Hz $^{-1}$)
-24
-25
-26
-27
10000
8000
6000
4000
3000
Wavelength (Å)
Log F_λ (erg cm $^{-2}$ s $^{-1}$ Hz $^{-1}$)
-24
-25
-26
-27
10000
8000
6000
4000
3000
Wavelength (Å)

FIG. 8

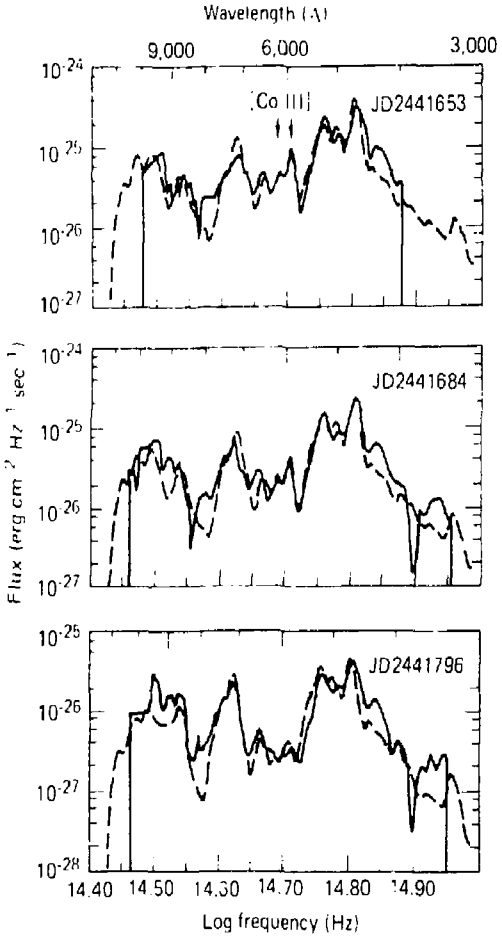
Wavelength (Å)
9,000
6,000
3,000
[Co III]
JD2441653
JD2441684
JD2441796
Flux (erg cm⁻² Hz⁻¹ sec⁻¹)
Log frequency (Hz)
14.40
14.50
14.30
14.70
14.80
14.90

FIG. 9

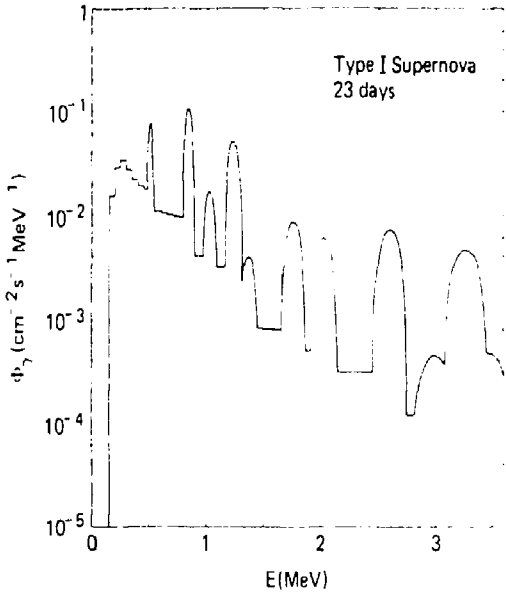
Type I Supernova
23 days
Φ_γ (cm^{-2}s^{-1}MeV^{-1})
1
10^{-1}
10^{-2}
10^{-3}
10^{-4}
10^{-5}
0
1
2
3
E(MeV)

FIG. 10

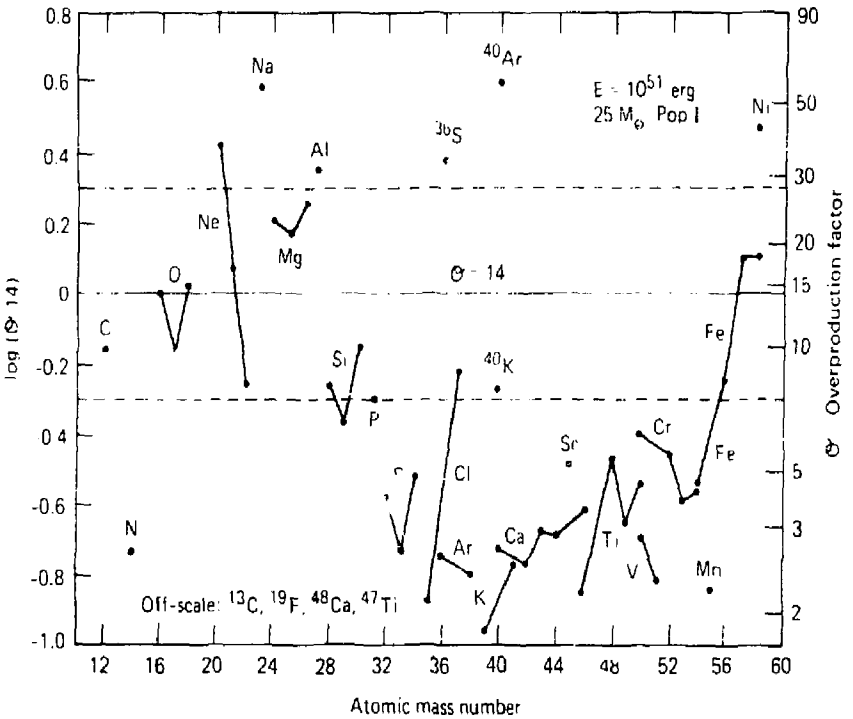
E = 10^51 erg
25 M⊙ Pop I
Θ = 14
Off-scale: 13C, 19F, 48Ca, 47Ti
log (Θ/14)
Θ Overproduction factor
Atomic mass number
Na
40Ar
Ni
36S
Al
Ne
Mg
O
C
Si
P
40K
Fe
Cr
Sr
Cl
Ar
Ca
Ti
V
Mn
K
N

FIG. 11

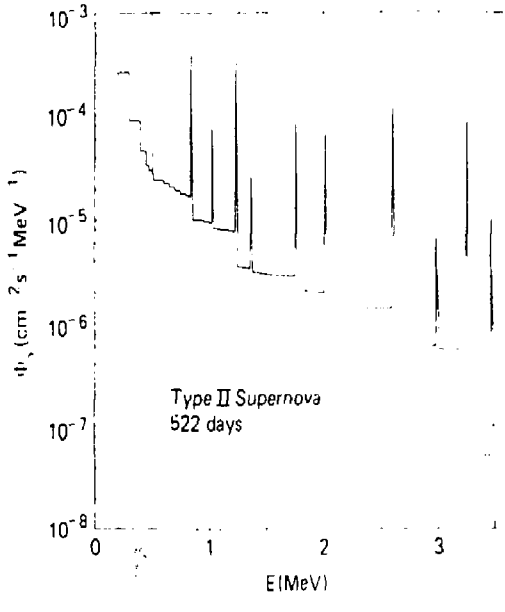
10^{-3}
10^{-4}
10^{-5}
10^{-6}
10^{-7}
10^{-8}
Φ_ν (cm $^{-2}$s $^{-1}$MeV $^{-1}$)
Type II Supernova
522 days
0
1
2
3
E(MeV)

FIG. 12

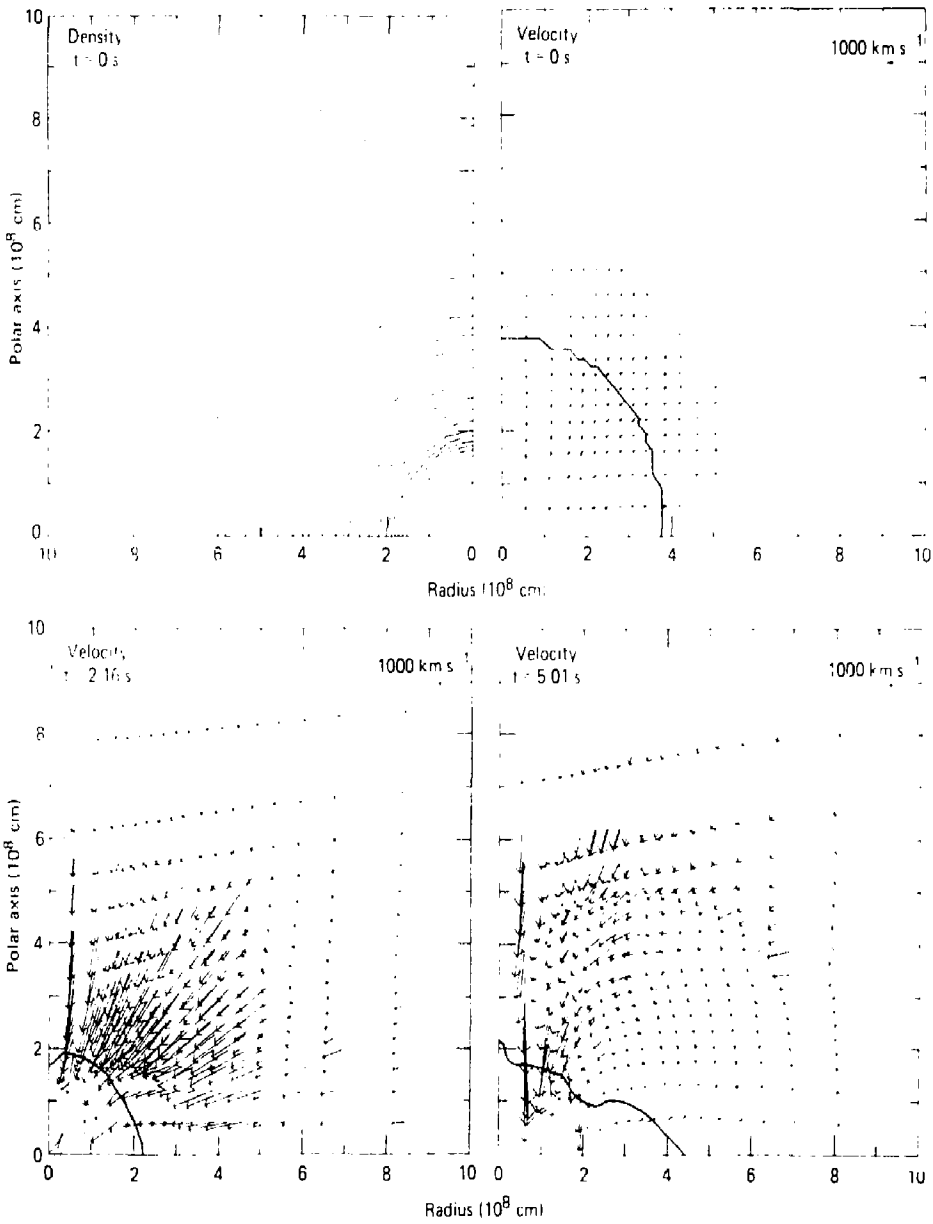
Density
t = 0 s
Velocity
t = 0 s
1000 km s⁻¹
Velocity
t = 2.16 s
1000 km s⁻¹
Velocity
t = 5.01 s
1000 km s⁻¹
Polar axis (10⁸ cm)
Radius (10⁸ cm)

FIG. 13

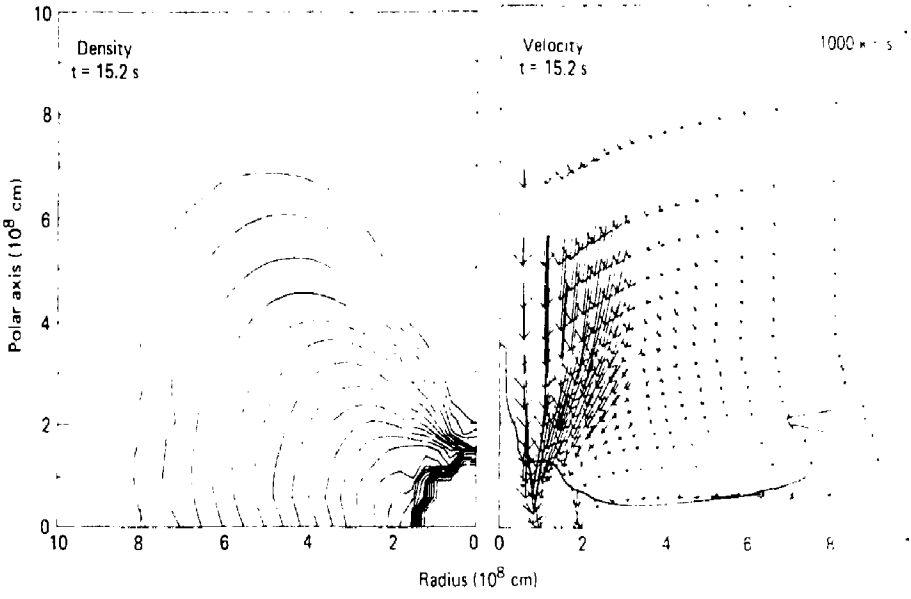
Density
t = 15.2 s
Velocity
t = 15.2 s
1000 km s
Polar axis (10^8 cm)
Radius (10^8 cm)
10
8
6
4
2
0
0
2
4
6
8

FIG. 14